



Application of catalytic wet peroxide oxidation for sunscreen agents breakdown

Neus Lopez-Arago^{*}, Amanda Dominguez, Macarena Munoz^{*}, Zahara M. de Pedro, Jose A. Casas

Chemical Engineering Department, Universidad Autónoma de Madrid, Ctra. Colmenar km 15, Madrid 28049, Spain

ARTICLE INFO

Keywords:

Sunscreen agents
Benzophenone-3 (BP-3)
4-aminobenzoic acid (PABA)
CWPO
Reaction pathway
Ecotoxicity

ABSTRACT

Sunscreen agents are chemical compounds widely used nowadays for skin protection from UV sunlight. Recently, their ubiquitous occurrence in aquatic systems has been evidenced, which poses a high risk for the environment and human health as they are associated with endocrine disrupting activity, reproductive toxicity, and genotoxicity. In this work, the feasibility of an economically and environmentally friendly catalytic system based on the thermally modified natural magnetite and hydrogen peroxide ($\text{Fe}_3\text{O}_4\text{-R400}/\text{H}_2\text{O}_2$), has been evaluated for the degradation of two representative sunscreen agents: benzophenone-3 (BP-3) and 4-aminobenzoic acid (PABA) in wastewater. The experiments were conducted under circumneutral pH ($\text{pH}_0 = 5$), with temperature control (25°C). Both compounds ($500\ \mu\text{g L}^{-1}$) were successfully removed from water by using a relatively low catalyst concentration ($0.5\ \text{g L}^{-1}$) and the theoretical stoichiometric H_2O_2 dose for their complete oxidation ($\sim 2.3\ \text{mg L}^{-1}$). Afterwards, a complete operating condition study was performed with BP-3, given its predominant occurrence in fresh waters, analysing the influence of H_2O_2 dose ($1.2\text{--}4.6\ \text{mg L}^{-1}$), catalyst concentration ($0.1\text{--}0.5\ \text{g L}^{-1}$), and temperature ($25\text{--}45^\circ\text{C}$). From the evolution of the identified by-products, a reaction pathway was proposed according to which oxidation of BP-3 gives rise to several aromatic intermediates, which finally evolve to short-chain organic acids. The generation of such aromatic by-products led to a considerably ecotoxicity increase in the initial stages of the reaction, but non-toxic effluents were ultimately achieved. Notably, the mineralization yield reached was above 60%. As a proof of concept, the feasibility of the system was finally demonstrated in real water matrices (WWTP effluent and surface water).

1. Introduction

The ubiquitous occurrence of micropollutants in all kinds of water bodies like lakes, rivers, oceans, and groundwater represents a serious environmental issue nowadays [1–3]. Among these micropollutants, sunscreen agents have been widely found in such compartments, posing a relevant risk for both human health and ecosystems given their endocrine disrupting activity, reproductive toxicity, and genotoxicity [4–6]. This is exacerbated by the high octanol/water partition coefficient values (k_{ow}) of most organic UV filters, making them prone to bioaccumulate in biota compared to other families of emerging pollutants [7]. For these reasons, sunscreen agents have been included in the latest Watch List (Decision 2022/1307) established by the European Commission for their monitoring and control. Two of the most used organic UV filters in our daily lives are benzophenone-3 (BP-3) and 4-aminobenzoic acid (PABA). These pollutants are commonly found in

plastic materials and in personal care products like sunscreens [8,9]. PABA is a UVB filter while BP-3 exhibits dual absorption capabilities in both the UVA and UVB range [10].

These compounds can reach the aquatic environment through either direct or indirect incorporation [9,11]. Tourism plays one of the most important roles in the direct transfer of sunscreen agents into water bodies, particularly in the coastal regions. Nevertheless, the contamination of fresh waters by UV-filters mainly occurs through indirect incorporation, being Wastewater Treatment Plants (WWTPs) a significant source of such compounds [12,13]. As has been demonstrated for many other micropollutants like antibiotics, hormones or pesticides, sunscreen agents cannot be completely eliminated in WWTPs, as these facilities have not been designed for such goal. Accordingly, UV-filters commonly appear in WWTP discharges. For instance, concentrations of $270\ \text{ng L}^{-1}$ for BP-3 have been recently reported [14]. Given to its continuous introduction into the environment and its high persistence,

^{*} Corresponding authors.

E-mail addresses: neus.lopez@uam.es (N. Lopez-Arago), macarena.munoz@uam.es (M. Munoz).

<https://doi.org/10.1016/j.jece.2024.112410>

Received 4 January 2024; Received in revised form 2 March 2024; Accepted 4 March 2024

Available online 5 March 2024

2213-3437/© 2024 The Authors. Published by Elsevier Ltd. This is an open access article under the CC BY-NC license (<http://creativecommons.org/licenses/by-nc/4.0/>).

concentrations of up to 2430 ng L⁻¹ of BP-3 have been reported in a European lake [15]. The concentrations of PABA in water are significantly lower given its high hydrophobicity, being found at significant concentrations (132–170 ng g⁻¹) in WWTP sewage sludge [16].

In this context, the development of innovative technologies capable of effectively removing these persistent micropollutants from water is urgently required. Advanced Oxidation Processes (AOPs), based on the action of non-selective, highly reactive and *in-situ* generated hydroxyl radicals, appear as promising candidates for such goal as they have already proved their effectiveness for the removal of other kinds of micropollutants like pharmaceuticals or pesticides, among other [17, 18]. Nevertheless, to the best of our knowledge, they have been scarcely investigated for the degradation of sunscreen agents so far. Pan et al. (2018) recently investigated the degradation of BP-3 by thermally activated persulfate [19]. Complete degradation of the pollutant (0.26 mg L⁻¹) was achieved after 3 h reaction time, but it required the operation at 40 °C and the application of a relatively high persulphate concentration (127 mg L⁻¹). Consistent with these findings, Zhang et al. (2020) only achieved a 60% degradation of PABA (6.8 mg L⁻¹) in 80 min employing the non-activated peroxyosulphate process (152.2 mg L⁻¹) [20]. The application of photocatalysis for the removal of PABA has been also accomplished in recent works. Tsoumachidou et al. (2016) achieved complete degradation of this UVB filter (20 mg L⁻¹) after 2 h reaction time employing a 9 W UV-A lamp and using a TiO₂ concentration of 0.5 g L⁻¹, but also adding a H₂O₂ dose of 200 mg L⁻¹ [21]. Under softer conditions, Perillo et al. (2017) reported an almost complete removal (97%) of PABA (6.7 mg L⁻¹) in 2 h reaction time by using a concentration of 0.5 g L⁻¹ of ZnO nanorods as photocatalyst and a solar irradiance of 0.1 W cm⁻² [22].

All in all, previous literature in the field is characterized by the application of energy and high catalyst/oxidant concentrations to achieve complete degradation of UV-filters in relatively long reaction times. Furthermore, even more severe operating conditions are required when AOPs are applied for the treatment of real aqueous matrices due to the consumption of oxidizing radicals by organic matter and the scavenging of those radicals by inorganic ions like chloride, sulfate or bicarbonate [23,24]. Therefore, it is essential to continue the search for technologies capable of degrading these pollutants while avoiding an increase in costs and ensuring environmental sustainability in the treatment of real aqueous matrices. Catalytic Wet Peroxide Oxidation (CWPO) may play a leading role in this field due to its cost-effectiveness. The only work in the literature dealing with the application of CWPO for BP-3 (2 mg L⁻¹) removal was based on the use of a Cu-Mn catalyst (100 mg L⁻¹) and a H₂O₂ concentration of 34 mg L⁻¹, not achieving its complete removal after 4 h reaction time (81.5% conversion) [25]. The application of natural magnetite as catalyst could lead to more promising results in terms of both activity and stability. In our previous contributions, we demonstrated that the catalytic system based on natural magnetite and hydrogen peroxide is extraordinarily active and reasonably stable in the degradation of different micropollutant families like pharmaceuticals, hormones and neonicotinoid and azolic pesticides [18,26].

In this work, the feasibility of CWPO promoted by the Fe₃O₄-R400/H₂O₂ catalytic system for the removal of two representative sunscreen agents, BP-3 and PABA is evaluated. Once confirmed the activity and stability of the catalytic system for the removal of both species, a complete operating condition study was conducted using BP-3 due to its ubiquitous occurrence in the aquatic environment. For such goal, the influence of H₂O₂ dose (1.2–4.6 mg L⁻¹), catalyst concentration (0.1–0.5 g L⁻¹), and operating temperature (25–45 °C) were systematically evaluated. Additionally, both the reaction by-products and ecotoxicity were followed along reaction to prove the feasibility of the system, not only for the removal of the target compound but also for assuring the obtention of non-toxic effluents at the end of the treatment. On the basis of these results, a reaction pathway for BP-3 degradation by CWPO was accordingly proposed. As a proof of concept, the effectiveness of the catalytic system was finally demonstrated using a WWTP

effluent as reaction matrix.

2. Materials and methods

2.1. Materials

The sunscreen agents, BP-3 and PABA, both of analytical grade quality, were purchased by Sigma-Aldrich. Hydrogen peroxide (33% wt.), nitric acid (65%), hydroxylamine (> 99%), formic acid (98%) and 1,10-phenantroline (> 99%) were also sourced from Sigma-Aldrich. Methanol (≥ 99%) was provided by Scharlab. All reagents were used as received without any additional purification step. Magnetite was obtained from Marphil S.L. (Spain) (ref: 50121500). Deionized water was employed to carried out all the experiments unless otherwise specified. Table 1 compiles the main properties of the micropollutants studied in this work.

2.2. Catalyst preparation and characterization

In our prior research, it was identified that natural magnetite modification by thermal reduction significantly enhanced its effectiveness while ensuring reasonable stability [28]. Therefore, before conducting the CWPO experiments, magnetite was thermally treated as described elsewhere [28]. Briefly, natural magnetite was reduced with a diluted H₂ flow (250 NmL min⁻¹ of 25 vol% H₂ in N₂) at 400 °C for 3 h. In short, the material had an iron content of 73% wt., surface area of 7 m² g⁻¹, and particles with an average diameter of 0.2 μm. It is noteworthy that the solid consisted exclusively of crystalline magnetite, exhibiting strong magnetic properties (81.5 emu g⁻¹) [17].

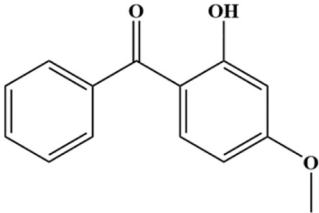
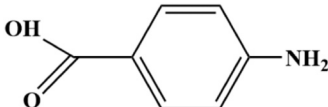
2.3. Experimental procedure

CWPO experiments were carried in a 500 mL glass batch reactor. The process was operated under ambient conditions (1 atm, 25 °C) and continuous stirring (750 rpm). The reaction volume was established at 450 mL. The initial pH was adjusted to 5 by HNO₃ (1 M), based on previous research confirming the optimal of this pH for this catalytic system considering both the efficiency on the decomposition of H₂O₂ as well as the possible agglomeration of magnetite [29]. The initial concentration of the UV-filters was set at 500 μg L⁻¹, which is higher than the typical level found in wastewater or other aquatic environments [30], but allowed for precise quantification of the micropollutants. It should be noted that the detection limit for the micropollutants in the HPLC-UV was around 5 μg L⁻¹ and thus, complete elimination of the micropollutants at ppb level was ensured. Unless otherwise indicated, the stoichiometric concentration of H₂O₂ required for complete oxidation of the target pollutants (Table 1) was employed along with a catalyst concentration of 0.5 g L⁻¹ of Fe₃O₄-R400. Those concentrations were selected taking into account previous contributions where the application of this catalytic system for a wide range of micropollutants was tested [17,26,28]. An additional set of experiments was carried to better follow the evolution of the intermediates along reaction as well as to assess the changes on the ecotoxicity of the reaction medium. For such goal, the initial concentration of BP-3 was established at 3.5 mg L⁻¹ and the H₂O₂ dose at 20% of the stoichiometric amount. Preliminary adsorption experiments were carried out in the absence of H₂O₂, but this contribution was discarded as micropollutant removal was below 10%. Additionally, blank experiments in the absence of catalyst were performed, resulting in negligible conversion of the target pollutants (<4%). The performance of the catalytic system for the removal of sunscreen agents was finally evaluated using a real WWTP effluent as reaction matrix. All experiments were conducted in triplicate.

2.4. Analytical methods

The progress of CWPO trials was followed by periodically

Table 1Main properties of the solar agents tested and H₂O₂ theoretical stoichiometric dose for their complete oxidation.

	Benzophenone – 3 (BP – 3)	4 – aminobenzoic acid (PABA)
Structural formula		
Chemical formula	C ₁₄ H ₁₂ O ₃	C ₇ H ₇ NO ₂
CAS number	131-57-7	150-13-0
Molecular weight (g mol ⁻¹)	228.2	137.1
pK _a ^{a,b}	8.06	¹ 2.42 ² 4.85
Log k _{ow} ^c	3.79	0.68
Reaction	C ₁₄ H ₁₂ O ₃ + 31 H ₂ O ₂ → 37 H ₂ O + 14 CO ₂	C ₇ H ₇ NO ₂ + 18 H ₂ O ₂ → 21 H ₂ O + 7CO ₂ + HNO ₃
Stoichiometric H ₂ O ₂ dosage (mg L ⁻¹) ^d	2.3	2.2

^a [27], ^b[20], ^c [11]^d Theoretical stoichiometric amount of H₂O₂ referred to an initial concentration of 500 μg L⁻¹.

withdrawing samples from the reactor. The catalyst was instantaneously separated by the application of a magnet and subsequently analyzed. The concentration of sunscreen agents was quantified by HPLC-UV (Shimadzu, Prominence-I model, LC-2030 C LT) using an Agilent Eclipse Plus C18 column (15 cm length, 4.6 mm diameter) as stationary phase. A mixture of methanol and ultrapure water with 0.1% of formic acid (66:34 (v/v)) and a mixture of methanol and acetic acid (75 mM) (40:60 (v/v)) were used for BP-3 and PABA, respectively. The analyses were performed at 289 nm and 264 nm for BP-3 and PABA, respectively.

The identification of the aromatic by-products formed along BP-3 reaction at high initial concentration (3.5 mg L⁻¹) was performed by LC/MS (TimsTPF Pro, Bruker) equipped with a quadrupole detector. In this case, a Zorbax Extend C18 column (4.6 mm diameter and 15 cm length) was used. A mixture of water (0.1% formic acid) (A) and acetonitrile (B) was used as mobile phase in a gradient method (t=0, % B=10; t=15, %B=100; t=30, %B=10). The acquisition and processing of the data was performed with the DataAnalyst 6.0 software.

An ion chromatograph Metrohm 883 IC Plus was used to quantify short-chain organic acids in final CWPO effluents. For the analysis, a Metrosep A supp 5–250 column (25 cm length, 4 mm internal diameter) served as stationary phase and an aqueous solution of Na₂CO₃ (3.2 mM) and NaHCO₃ (1 mM) as mobile phase. Total organic carbon (TOC) was determined with a TOC analyzer (Shimadzu TOC V_{SCH}, Kyoto, Japan). Simultaneously, the dissolved iron concentration was quantified through the colorimetric *o*-phenantroline method [31]. The spectrophotometer used for this purpose was the Shimadzu UV-VIS 2100.

2.5. Ecotoxicity tests

Vibrio fischeri was employed to evaluate both the ecotoxicity of the target compounds and the reaction effluents. The standardized Microtox® toxicity test (1998, ISO 11348–3) was followed using a M500 Microtox Analyzer. Prior conducting the ecotoxicity tests, the osmotic pressure of the samples was adjusted employing a 2% sodium chloride solution, and the pH was carefully set within the range of 6.0–8.0. The experimental tests were conducted at a controlled temperature of 15 °C. Subsequently, the determination of the half maximum effective concentration (EC₅₀) was undertaken for each sunscreen agent. The EC₅₀ value represents the concentration (expressed in mg L⁻¹) of the substance that induces a 50% reduction in the intensity of light emitted by the marine bacterium after exposing it to the sample during 15 min. In complex samples, IC₅₀ is calculated, representing the dilution percentage at which a 50% reduction in light emission occurs. Both EC₅₀ and IC₅₀ values exhibit an inverse correlation with ecotoxicity, expressed in

toxicity units (TU). This relationship is described by Eq. (1), where C₀ denotes the concentration of the compound used to determine its EC₅₀ value.

$$TU = \frac{C_0 \text{ (mg L}^{-1}\text{)}}{EC_{50}} = \frac{100}{IC_{50}} \quad (1)$$

3. Results and discussion

3.1. Sunscreen agents breakdown by CWPO

Fig. 1 shows the time-course of BP-3 and PABA upon CWPO process. These experiments were performed using a catalyst concentration of 0.5 g L⁻¹, and the stoichiometric dose of H₂O₂. As can be seen, both compounds were completely removed in 2 h reaction time, although different disappearance rates were appreciated. BP-3 exhibited the highest degradation rate, achieving complete removal in 15 min, while total elimination of PABA required up to 2 h. The evolution of the pollutants was successfully described by a pseudo-first order kinetic

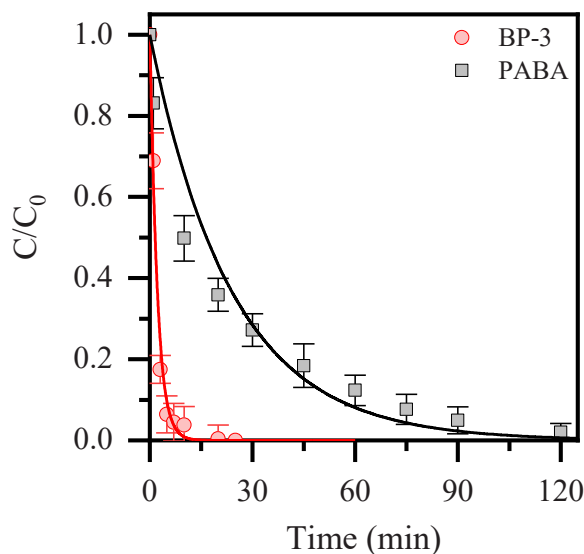


Fig. 1. Evolution of sunscreen agents (individually treated) upon CWPO ([Pollutant]₀ = 500 μg L⁻¹, [H₂O₂]₀ = stoichiometric concentration; [Fe₃O₄-R400]₀ = 0.5 g L⁻¹; pH₀ = 5; T = 25 °C). Experimental (symbols) and model fit (solid lines).

equation, obtaining rate constant values of 0.47 min^{-1} and 0.04 min^{-1} for BP-3 and PABA, respectively. These values can be compared to those obtained in our previous works for other micropollutants included in the EU Watch List. It is worth noting that, among all the micropollutants tested so far, BP-3 stand out for showing the highest kinetic constant value, indicating that it is particularly reactive towards CWPO [26]. On the opposite, the rate constant value of PABA aligns with the most resistant azole pesticides towards this oxidation treatment [26]. Remarkably, the catalyst exhibited notable stability under all investigated operating conditions, consistently ensuring that the dissolved iron concentration in the effluent remained below 0.5 mg L^{-1} (1% wt.) in all cases. All in all, these findings confirm that the CWPO process employing the $\text{Fe}_3\text{O}_4\text{-R400}/\text{H}_2\text{O}_2$ catalytic system yields efficiencies in sunscreen agent removal comparable to those reported for other micropollutant families included in the EU Watch Lists. Furthermore, this study demonstrated promising outcomes compared to results obtained from alternative oxidation processes reported in the literature for the removal of sunscreen agents. For instance, the complete degradation of BP-3 through thermally activated persulfate treatment at 40°C required a 3 h reaction time combined with a high persulfate concentration [19]. Likewise, Zhang et al. reported a conversion value of only 60% within 80 min when using non-activated peroxymonosulfate for PABA oxidation [20].

The differences found in the reactivity of the sunscreen agents towards CWPO can be directly associated with their chemical structures. As can be seen in Table 1, BP-3 is a substituted benzophenone with a hydroxyl group in the *ortho* position, and a methoxy group in the *para* position. Hydroxyl radicals react with aromatic compounds, being BP-3 a very good candidate for this kind of interaction. These radicals may abstract H from C-H and O-H bonds and can be added to aromatic rings [32]. Accordingly, practically all positions of BP-3 are susceptible to be oxidized, which explains that its oxidation rate is among the highest ones achieved in the removal of micropollutants from water by this catalytic system [26]. On the opposite, PABA, formed by a single benzene ring substituted with an amino group and a carboxyl group in its *para* position, is clearly lower reactive towards hydroxyl radical attack. Even though the amino group can stabilize the aromatic ring, its electron-donor capacity is considerably weaker than the hydroxyl group. In fact, previous works in the literature have demonstrated that derivatives of aniline exhibit great resistance towards advanced oxidation and may require intensified operating conditions to achieve significant removal efficiencies [33].

3.2. Operating condition study

Given its predominant occurrence in both WWTP effluents and fresh waters, BP-3 was selected as target pollutant to perform the operating condition study. In first place, the impact of the catalyst concentration and H_2O_2 dose on the oxidation rate of the sunscreen agent was evaluated (Fig. 2). Fig. 2a shows the evolution of BP-3 upon CWPO using different $\text{Fe}_3\text{O}_4\text{-R400}$ catalyst concentrations ($0.1 - 0.5 \text{ g L}^{-1}$) and the stoichiometric amount of H_2O_2 . As can be observed, higher catalyst loads led to a faster oxidation of the solar agent. Increasing the catalyst concentration from 0.1 to 0.5 g L^{-1} allowed to reduce the reaction time required to achieve the complete conversion of BP-3 from 45 to 15 min. Pseudo-first order kinetic constant values of 0.10 , 0.21 and 0.47 min^{-1} were obtained for the catalyst concentrations of 0.1 , 0.25 and 0.5 g L^{-1} , respectively. These results can be explained by the fact that more catalytic active sites are available for the decomposition of hydrogen peroxide into hydroxyl radicals, thus increasing the oxidation rate of the pollutant. Furthermore, it must be noted that the rate constant values increased linearly with increasing the catalyst concentration, which proves that the reaction proceeded without external mass transfer limitations (see Figure S1 of the Supplementary Material).

Hydrogen peroxide is usually identified as the main operating cost of Fenton-like technologies and thus, the optimization of its consumption is crucial for practical implementation of CWPO at WWTPs [34,35]. Fig. 2b shows the evolution of BP-3 at different H_2O_2 doses corresponding to 50%, 100%, 150% and 200% of the stoichiometric amount (1.15 , 2.31 , 3.46 and 4.62 mg L^{-1} , respectively). All experiments were performed with a catalyst concentration of 0.1 g L^{-1} . Clearly, H_2O_2 concentration played a significant role on the extension of the reaction. The H_2O_2 dose below the theoretical stoichiometric amount for the complete oxidation of BP-3 did not allow to achieve the complete conversion of the pollutant even after 1 h reaction time, while H_2O_2 doses at or above that threshold value allowed to reach the complete removal of the target pollutant in less than 45 min. H_2O_2 concentration also affected the oxidation rate, observing a marked increase with increasing the dose from 1.2 to 3.2 mg L^{-1} , while higher increase up to 4.6 mg L^{-1} did not allow to further rise the oxidation rate. This fact can be attributed to the occurrence of an excessive concentration of H_2O_2 , where the oxidant can act as $\text{HO}\cdot$ scavenger when iron redox cycle in the catalyst is completed yielding $\text{HOO}\cdot$ that reacts with $\text{HO}\cdot$ resulting in molecular oxygen, leading to the so-called termination reactions between both radicals [32]. The pseudo-first order rate constant values obtained were 0.03 , 0.10 , 0.19 and 0.22 min^{-1} for 50%, 100%, 150% and 200% of the

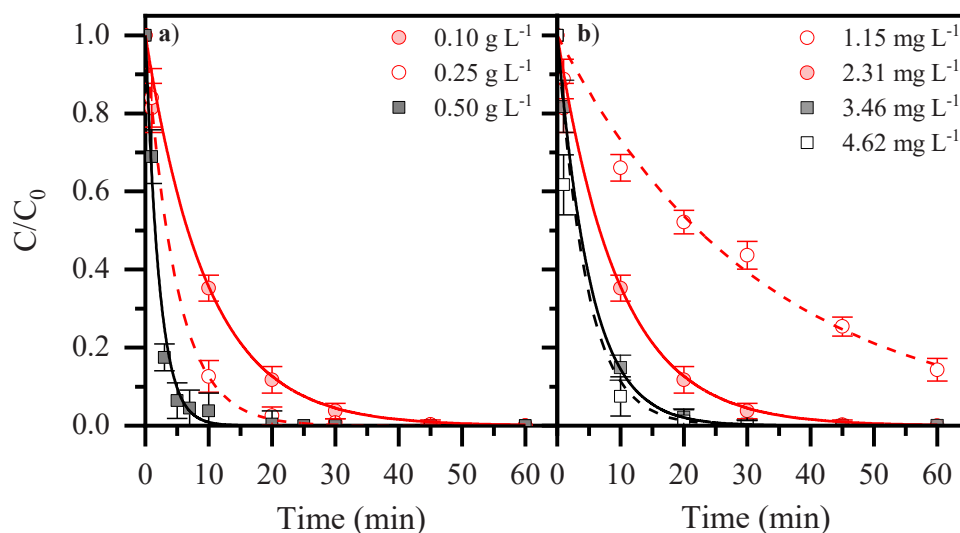


Fig. 2. Impact of the operation conditions (a: catalyst concentration ($0.1 - 0.5 \text{ g L}^{-1}$), b: H_2O_2 concentration ($1.15 - 4.62 \text{ mg L}^{-1}$)) on the oxidation of BP-3 ($[\text{BP-3}]_0 = 500 \text{ }\mu\text{g L}^{-1}$; $\text{pH}_0 = 5$; $T = 25^\circ\text{C}$). Experimental (symbols) and model fit (solid lines).

stoichiometric amount, respectively. These results are in good agreement with previous works in the literature, suggesting that continuous increase in oxidant concentration does not necessarily lead to an increase of the process efficiency [29,36]. Based on these results, the stoichiometric amount of H_2O_2 was selected to continue with the research study.

The influence of the operating temperature on the evolution of BP-3 upon CWPO can be seen in Fig. 3. These experiments were conducted using the stoichiometric H_2O_2 dose and a catalyst concentration of 0.1 g L^{-1} . As expected, a positive correlation was observed between the operating temperature and the degradation rate of BP-3. Pseudo-first order kinetic constant values of 0.10, 0.21 and 0.52 min^{-1} were obtained for temperatures of 25, 35 and $45 \text{ }^\circ\text{C}$, respectively. The activation energy was calculated from the Arrhenius equation, obtaining a value of 63.5 kJ mol^{-1} . This value is in the same order of magnitude as those reported in the literature for the CWPO with other types of micro-pollutants, as well as with conventional contaminants such as phenols or dyes [17,37].

To evaluate the reusability of the catalyst, three consecutive oxidation runs were performed using the same catalyst sample under the operating conditions previously selected ($[\text{BP-3}]_0 = 500 \text{ } \mu\text{g L}^{-1}$; $[\text{H}_2\text{O}_2]_0 = 2.3 \text{ mg L}^{-1}$; $[\text{Fe}_3\text{O}_4\text{-R400}]_0 = 0.1 \text{ g L}^{-1}$; $\text{pH}_0 = 5$; $T = 25 \text{ }^\circ\text{C}$). Although a decrease on the oxidation rate of the pollutant was found, more than 80% conversion was achieved after 1 h reaction time after the third oxidation run (Figure S2 of the Supplementary Material). Deactivation can be explained neither by the leaching of iron (below 0.5 mg L^{-1} after each run) nor by the presence of carbonaceous deposits (carbon content below 0.1%wt.) but by the partial oxidation of the catalyst surface during reaction. This is consistent with a previous contribution where the activity of modified natural magnetite by thermal oxidation and reduction treatments was investigated [28].

3.3. Degradation pathway

To elucidate the reaction pathway of BP-3 upon CWPO, a new set of experiments was conducted using a significant sub-stoichiometric H_2O_2 dose (20% of theoretical stoichiometric amount). These operating conditions allowed the identification of the intermediates formed along the initial stages of AOPs in previous works [17,38,39]. The evolution of the aromatic intermediates was followed by HPLC-UV, obtaining the curves

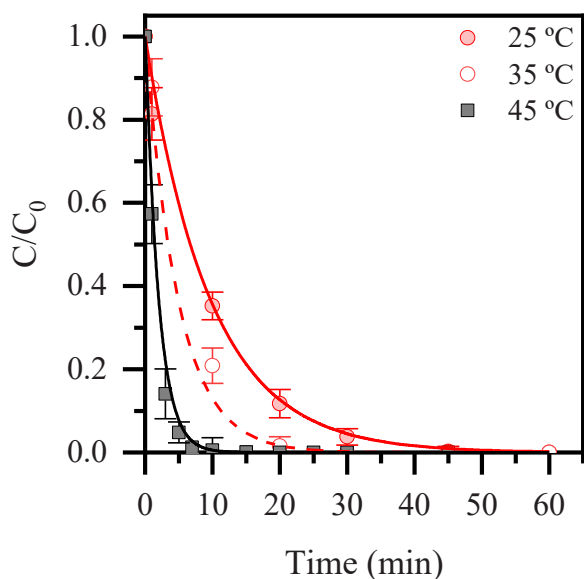


Fig. 3. Effect of temperature on the degradation of BP-3 upon CWPO with $\text{Fe}_3\text{O}_4\text{-R400}$ ($[\text{BP-3}]_0 = 500 \text{ } \mu\text{g L}^{-1}$; $[\text{H}_2\text{O}_2]_0 = 2.3 \text{ mg L}^{-1}$; $[\text{Fe}_3\text{O}_4\text{-R400}]_0 = 0.1 \text{ g L}^{-1}$; $\text{pH}_0 = 5$). Experimental (symbols) and model fit (solid lines).

collected in Fig. 4. As can be observed, the decrease in the concentration of the target pollutant primarily led to the generation of a variety of aromatic byproducts.

With the aim of identifying the main intermediates formed along reaction, the previous samples were also analysed by LC/MS. Based on these results, the reaction pathway shown in Fig. 5 was proposed. The reaction is primarily initiated by the hydroxylation of the parent molecule, leading to the formation of higher molecular weight intermediates, which commonly constitutes the first stage in the application of Fenton-based technologies for aromatic compounds removal [12,40]. Intermediates formed by the addition of one, two and three hydroxyl groups were identified (m/z of 244, 260 and 276, respectively). Apart from direct addition of hydroxyl groups into the molecule, hydroxyl radicals can substitute the methoxy group of BP-3, resulting in the generation of 2,4-dihydroxybenzophenone ($m/z = 214$, I_1 in Fig. 5), also known as benzophenone-1 (BP-1) [12]. The generation of such intermediate has been also reported in different kinds of advanced oxidation treatments like persulfate oxidation [19], photoelectron-Fenton [41], or hybrid system sono-electro-Fenton [42]. Similarly, this hydroxylation route was also observed by Zou et al. (2021) in the degradation of BP-1 by zero valent iron powder-activated persulfate [43]. Moreover, reaction of hydroxyl radical with a hydrogen substituent and a near hydroxyl groups leads to the formation of an ether group within the central ring, giving rise to the I_4 by-product ($m/z = 258$). This phenomenon is consistent with the cyclation pathway reported by Zou et al. (2021) in the degradation of BP-1 by zero valent iron powder-activated persulfate [43], and also aligns with observations made by Gong et al. (2015), who noted a comparable behavior during the degradation this pollutant using the UV/ H_2O_2 process [12]. Further hydroxyl radical attack would also lead to bond cleave leading to the generation of intermediates of one aromatic ring like phenol or benzoic acid, as reported by Zou et al. (2021) in the degradation of BP-1 by zero valent iron powder-activated persulfate [43]. Nevertheless, simple aromatic compounds were not detected in our work, possibly due to their fast oxidation under the operating conditions tested and thus. In the current work, breakage of the abovementioned intermediates and their ring-opening was found, leading to the generation of short-chain organic acids. This fact was evidenced by analysing the reaction effluent achieved in the CWPO of BP-3 at the conditions of Fig. 1, using the stoichiometric dose of H_2O_2 and a catalyst concentration of 0.5 g L^{-1} , by ionic chromatography. The presence of maleic, acetic, oxalic, and formic acids as reaction products was confirmed. These acids are well-known products obtained in the degradation of aromatic compounds by AOPs, particularly by Fenton-based processes [17,44]. It must be noted that all the aromatic intermediates followed by HPLC-UV were completely removed from the reaction medium when the reaction was performed using the stoichiometric dose of H_2O_2 (see Figure S3 of the Supplementary Materials) and thus, short-chain organic acids are the final residual products present in the effluent. Notably, a substantial mineralization yield of the effluent was achieved (~60%).

3.4. Ecotoxicity study

It is well-known that the application of AOPs for micropollutants removal can lead to the formation of higher toxicity intermediates along reaction and, in some cases, final effluents can still be toxic [38,45]. Accordingly, once confirmed the effectiveness of CWPO for the removal of BP-3, the evolution of ecotoxicity along reaction was evaluated. For such goal, a standardized ecotoxicity assay based on the use of the bioluminescent bacterium *Vibrio fischeri* was employed. The obtained EC_{50} value for BP-3 was 2.0 mg L^{-1} . To the best of our knowledge, the EC_{50} of this compound using *Vibrio fischeri* as target organism has not been previously reported in the literature. Anyway, this result is in good agreement with the EC_{50} values reported for other kinds of organisms. For instance, EC_{50} values of $\sim 2.0 \text{ mg L}^{-1}$ (48 h) were obtained for *Daphnia magna* [46,47]. Similarly, LC_{50} values of 3.9 mg L^{-1} (96 h) were

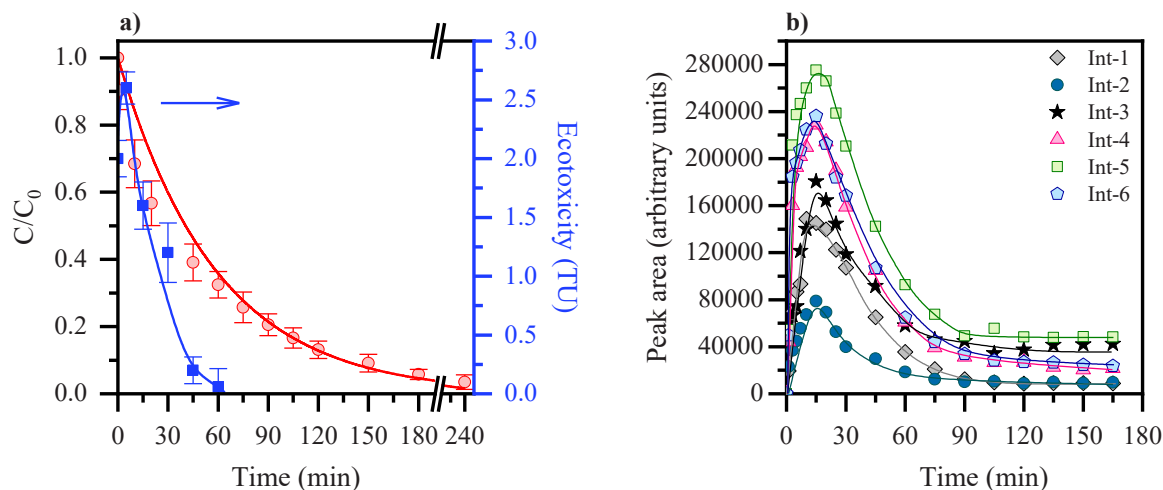


Fig. 4. Evolution BP-3 and ecotoxicity (a) and aromatic by-products (b) upon CWPO ($[\text{BP-3}]_0 = 3.5 \text{ mg L}^{-1}$; $[\text{Fe}_3\text{O}_4\text{-R400}] = 0.1 \text{ g L}^{-1}$; $[\text{H}_2\text{O}_2]_0 = 3.2 \text{ mg L}^{-1}$; $\text{pH}_0 = 5$; $T = 25 \text{ }^\circ\text{C}$).

obtained using *Brachydanio rerio* as a bioindicator, while an EC_{50} of 2.9 mg L^{-1} (96 h) was determined for *Chlorella vulgaris* [48]. It is worth noting that this sunscreen agent exhibits higher toxicity compared to other UV filters within the benzophenone family [49]. In fact, the primary factor influencing the toxicity of sunscreen filters is the electrostatic effect, and BP-3 contains electron-donating groups such as -OH group located at the *ortho*- position and the -OCH₃ group positioned at the *para*- position of the aromatic ring [46,49].

To better follow the ecotoxicity along reaction, the experiment was carried out under the operating conditions of Fig. 4, i.e., using a higher initial concentration of the pollutant (3.5 mg L^{-1}) and the sub-stoichiometric dose of H_2O_2 (3.2 mg L^{-1}). Fig. 4a shows the evolution of both the concentration of the sunscreen agent and ecotoxicity along the CWPO reaction. As shown in Fig. 4a, the initial ecotoxicity value exhibited a significant increase within the initial 5 minutes, reaching a peak of 2.6 TU. However, after surpassing this threshold value, the ecotoxicity value suffered a sharp decline, resulting in a non-toxic effluent after 60 minutes. As can be seen in Fig. 4b, the evolution of the aromatic intermediates (measured by HPLC-UV) closely followed the ecotoxicity data trend. This trend is consistent with the appearance of aromatic by-products, which reached their highest concentration at 15 min reaction time. These findings emphasize that the by-products generated during the oxidation process are significantly more toxic than the parent compound. In fact, as depicted in Fig. 4b, these intermediates were eliminated to a high extent at the end of the reaction and, consistently, the final effluent was non-toxic.

3.5. Operation in complex water matrices

In a real scenario, micropollutants would be part of a complex water matrix with co-existing organic and inorganic components that may greatly influence the efficiency of the CWPO process [24,50,51]. To evaluate such aspect, the feasibility of the catalytic system was tested using a WWTP effluent and surface water as reaction matrices. These aqueous matrices were spiked with BP-3 at a relatively representative concentration of $200 \text{ } \mu\text{g L}^{-1}$. To ensure the complete removal of the pollutant in reasonable reaction times, the reactions were conducted using a catalyst concentration of 0.5 g L^{-1} and a H_2O_2 dose of 5 mg L^{-1} . The characterization of both aqueous matrices is collected in Table 2, and the obtained results in the CWPO experiments are shown in Fig. 6.

As can be seen in Fig. 6, the oxidation rate of BP-3 was clearly lower when the reaction proceeded in the WWTP effluent instead of ultrapure water. In the case of surface water, a significantly lower impact on the oxidation rate of BP-3 was observed. The pseudo-first order rate constant

values obtained in these water matrices were 4.5 , 1.6 and 0.14 min^{-1} , for ultrapure water, surface water and WWTP effluent, respectively. These results can be explained by the occurrence of both organic and inorganic species in the real water matrices. It is widely recognized that $\text{HO}\cdot$ is a non-selective oxidant [52–54], so co-existing organic matter would clearly compete with BP-3 for the consumption of hydroxyl radicals. It must be noted that the concentration of TOC was 4.1 mg L^{-1} , which is 20 times the concentration of the micropollutant. Similarly, the occurrence of different inorganic species such as bicarbonates (directly related to the IC concentration of the real water matrices), chlorides, and sulfates could act as $\text{HO}\cdot$ scavengers [32]. The WWTP effluent exhibited a high concentration of Cl^- and inorganic carbon (Table 2), which could be the main responsible for the significant decrease on BP-3 oxidation rate. These findings are consistent with those recently reported by Ortiz et al. (2023), who investigated the impact of water composition on the degradation of cyanotoxins [55]. As the authors of this work indicated, the presence of chloride, sulfate and bicarbonate negatively affects the oxidation rate while phosphate and nitrate do not pose any significant impact. Although chloride and sulfate could lead to the generation of their radical counterparts, they exhibit considerably lower oxidizing potential than hydroxyl radicals, leading to a decrease in the overall oxidation rate. All in all, it must be noted that CWPO was still effective even in the real WWTP effluent operating under ambient conditions and relatively low H_2O_2 and catalyst concentrations.

4. Conclusions

The $\text{Fe}_3\text{O}_4\text{-R400}/\text{H}_2\text{O}_2$ catalytic system has proved to be effective for the removal of sunscreen agents (BP-3 and PABA) from water. The reactivity of both pollutants towards CWPO was found to be dependent on their chemical structure. BP-3, containing two aromatic rings with hydroxyl and methoxy groups, was clearly more susceptible to oxidation than PABA, which showed more resistance given the presence of an amino group in its structure. The operating condition study conducted for BP-3 degradation, demonstrated the key role of catalyst concentration on the kinetics of the process and the predominant influence of H_2O_2 on the extension of the reaction. Catalyst concentration within the range of $0.1\text{--}0.5 \text{ g L}^{-1}$ and the stoichiometric dose of H_2O_2 allowed to ensure the complete oxidation of the sunscreen agents in short reaction times ($<1 \text{ h}$). The feasibility of the catalytic system was evidenced based on the evolution of by-products compounds and ecotoxicity along reaction. A sharp ecotoxicity increase was achieved along the first stages of the reaction, consistent with the generation of a wide range of aromatic intermediates. Notably, they were eliminated at the end of the

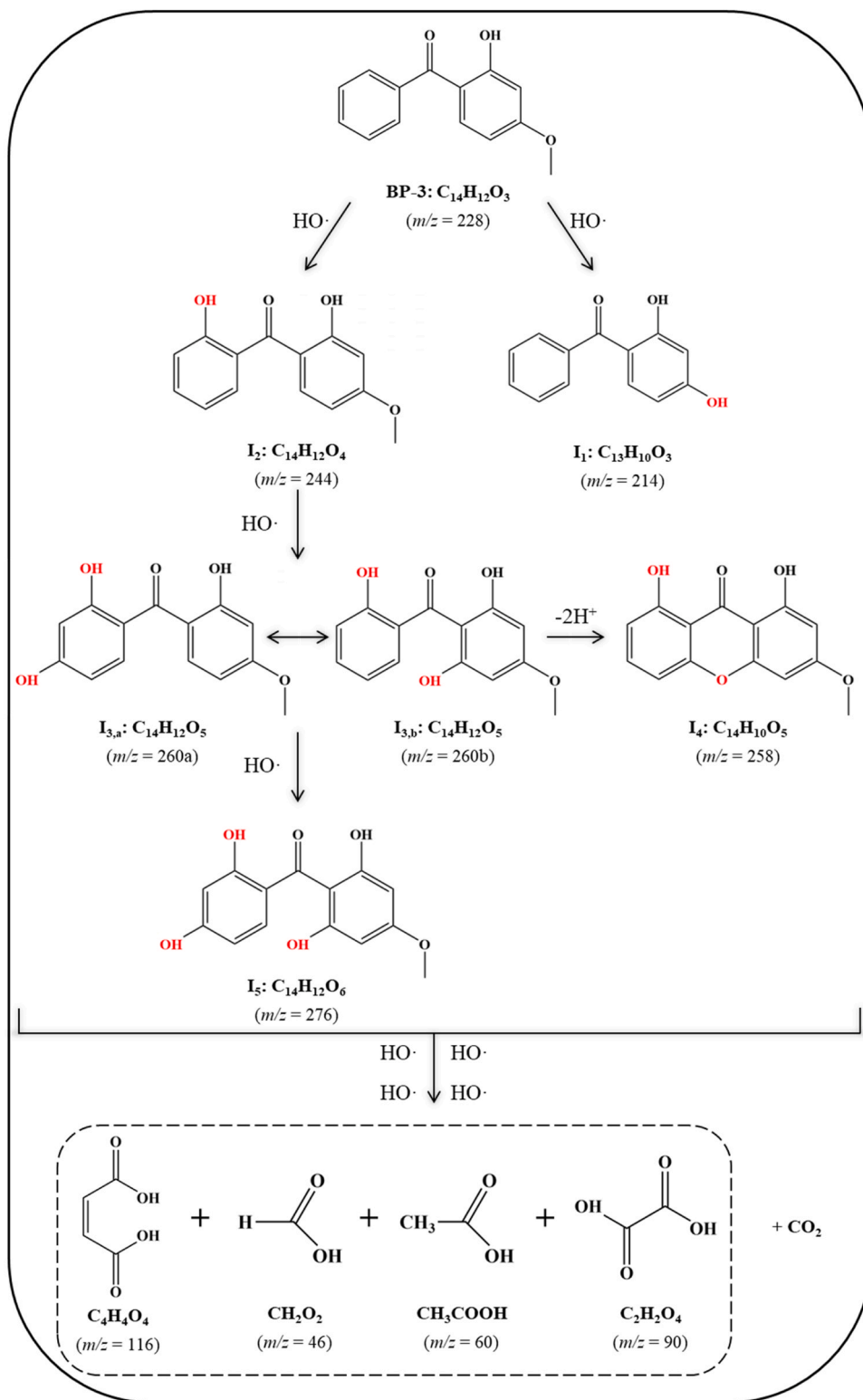


Fig. 5. Proposed reaction pathway for BP-3 degradation upon CWPO.

treatment, giving rise to short-chain organic acids as reaction products and thus, non-toxic effluents. Furthermore, mineralization yield reached up to 60%. As a proof of concept, the process was tested with a real water matrix (WWTP effluent) and successfully achieved the complete removal of BP-3. However, the oxidation rate of the pollutant was noticeably impacted by the presence of co-existing species, highlighting the importance of optimizing this system in practical applications.

CRediT authorship contribution statement

Zahara M. de Pedro: Writing – review & editing, Supervision, Project administration, Funding acquisition, Conceptualization, Methodology. **Jose A. Casas:** Writing – review & editing, Supervision, Project administration, Funding acquisition, Conceptualization, Methodology. **Amanda Dominguez:** Methodology, Investigation. **Macarena Munoz:**

Table 2
Main characteristics of real water matrix tested.

Parameter	Secondary WWTP effluent	Surface Water
pH	7.3	7.2
TOC (mg L ⁻¹)	4.3	2.0
IC (mg L ⁻¹)	22.5	1.5
Conductivity (μS cm ⁻¹)	525	22.7
Cl ⁻ (mg L ⁻¹)	191.3	2.5
NO ₃ ⁻ (mg L ⁻¹)	10.0	-
SO ₄ ²⁻ (mg L ⁻¹)	18.7	0.5
PO ₄ ³⁻ (mg L ⁻¹)	1.3	0.3

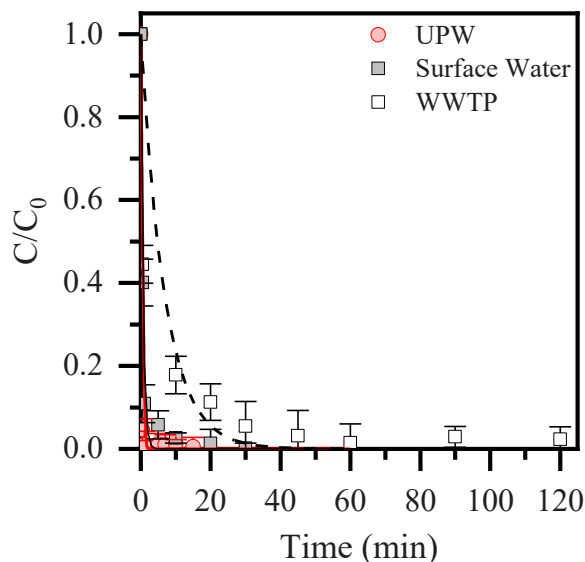


Fig. 6. Evolution of the BP-3 upon CWPO with Fe₃O₄-R400 in different water matrices ([BP-3]₀ = 200 μg L⁻¹; [H₂O₂]₀ = 5 mg L⁻¹; [Fe₃O₄-R400]₀ = 0.5 g L⁻¹; pH₀ = 5; T = 25 °C). Experimental (symbols) and model fit (solid lines).

Writing – review & editing, Writing – original draft, Supervision, Project administration, Funding acquisition, Conceptualization, Methodology. **Neus Lopez-Arago:** Writing – original draft, Visualization, Methodology, Investigation, Writing – review & editing.

Declaration of Competing Interest

The authors declare that they have no known competing financial interests or personal relationships that could have appeared to influence the work reported in this paper.

Data availability

Data will be made available on request.

Acknowledgments

This research has received support from the Spanish Ministry of Science and Innovation and AEI through the grants PID2019-105079RB-I00 and PID2022-139063OB-I00 funded by MCIN/AEI/10.13039/501100011033 and by ERDF A way of making Europe, and from the Community of Madrid through the grant P2018/EMT-4341. N. Lopez-Arago thanks for the FPI predoctoral grant (PRE2020-09452) funded by MCIN/AEI/ 10.13039/501100011033 and by ESF Investing in your future.

Appendix A. Supporting information

Supplementary data associated with this article can be found in the online version at doi:10.1016/j.jece.2024.112410.

References

- [1] X. Li, T. Tian, X. Shang, R. Zhang, H. Xie, X. Wang, H. Wang, Q. Xie, J. Chen, K. Kadokami, Occurrence and health risks of organic micro-pollutants and metals in groundwater of Chinese rural areas (Article), *Environ. Health Perspect.* 128 (2020) 107010, <https://doi.org/10.1289/ehp6483>.
- [2] T. Miyawaki, T. Nishino, D. Asakawa, Y. Haga, H. Hasegawa, K. Kadokami, Development of a rapid and comprehensive method for identifying organic micropollutants with high ecological risk to the aquatic environment, *Chemosphere* 263 (2021) 128258, <https://doi.org/10.1016/j.chemosphere.2020.128258>.
- [3] O. Golovko, A.L. Rehrl, S. Köhler, L. Ahrens, Organic micropollutants in water and sediment from Lake Mälaren, Sweden, *Chemosphere* 258 (2020) 127293, <https://doi.org/10.1016/j.chemosphere.2020.127293>.
- [4] P. Nicolopoulou-Stamati, L. Hens, A.J. Saso, Cosmetics as endocrine disruptors: are they a health risk? *Rev. Endocr. Metab. Disord.* 16 (2015) 373–383, <https://doi.org/10.1007/s11154-016-9329-4>.
- [5] J.A. Ruszkiewicz, A. Pinkas, B. Ferrer, T.V. Peres, A. Tsatsakis, M. Aschner, Neurotoxic effect of active ingredients in sunscreen products, a contemporary review, *Toxicol. Rep.* 4 (2017) 245–259, <https://doi.org/10.1016/j.toxrep.2017.05.006>.
- [6] S.L. Schneider, H.W. Lim, Review of environmental effects of oxybenzone and other sunscreen active ingredients, *J. Am. Acad. Dermatol.* 80 (2018) 266–271, <https://doi.org/10.1016/j.jaad.2018.06.033>.
- [7] D. Sánchez-Quiles, A. Tovar-Sánchez, Are sunscreens a new environmental risk associated with coastal tourism? *Environ. Int.* 83 (2015) 158–170, <https://doi.org/10.1016/j.envint.2015.06.007>.
- [8] A. Scheele, K. Sutter, O. Karatum, A.A. Danley-Thomson, L.K. Redfern, Environmental impacts of the ultraviolet filter oxybenzone, *Sci. Total Environ.* 863 (2023) 160966, <https://doi.org/10.1016/j.scitotenv.2022.160966>.
- [9] M. Chatzigianni, P. Pavlou, A. Siamidi, M. Vlachou, A. Varvaresou, S. Papageorgiou, Environmental impacts due to the use of sunscreen products: a mini-review, *Ecotoxicology* 31 (2022) 1331–1345, <https://doi.org/10.1007/s10646-022-02592-w>.
- [10] L. Azcona Barbed, *Protección solar. Actualización*, *Farm. Prof.* 17 (2003) 66–75.
- [11] A.J.M. Santos, M.S. Miranda, J.C.G. Esteves da Silva, The degradation products of UV filters in aqueous and chlorinated aqueous solutions, *Water Res.* 46 (2012) 3167–3176, <https://doi.org/10.1016/j.watres.2012.03.057>.
- [12] P. Gong, H. Yuan, P. Zhai, Y. Xue, H. Li, W. Dong, G. Mailhot, Investigation on the degradation of benzophenone-3 by UV/H₂O₂ in aqueous solution, *Chem. Eng. J.* 277 (2015) 97–103, <https://doi.org/10.1016/j.cej.2015.04.078>.
- [13] P. Gago-Ferrero, M. Badia-Fabregat, A. Olivares, B. Piña, P. Blázquez, T. Vicent, G. Caminal, M.S. Díaz-Cruz, D. Barceló, Evaluation of fungal- and photo-degradation as potential treatments for the removal of sunscreens BP3 and BP1, *Sci. Total Environ.* 427–428 (2012) 355–363, <https://doi.org/10.1016/j.scitotenv.2012.03.089>.
- [14] J. Margot, L. Rossi, D.A. Barry, C. Holliger, A review of the fate of micropollutants in wastewater treatment plants, *Wiley Interdiscip. Rev. Water* 2 (2015) 457–487, <https://doi.org/10.1002/WAT2.1090>.
- [15] R. Rodil, S. Schrader, M. Moeder, Non-porous membrane-assisted liquid-liquid extraction of UV filter compounds from water samples, *J. Chromatogr. A* 1216 (2009) 4887–4894, <https://doi.org/10.1016/j.chroma.2009.04.042>.
- [16] P. Gago-Ferrero, M.S. Díaz-Cruz, D. Barceló, Liquid chromatography-tandem mass spectrometry for the multi-residue analysis of organic UV filters and their transformation products in the aquatic environment, *Anal. Methods* 5 (2013) 355–366, <https://doi.org/10.1039/c2ay26115d>.
- [17] E. Serrano, M. Munoz, Z.M. de Pedro, J.A. Casas, Efficient removal of the pharmaceutical pollutants included in the EU Watch List (Decision 2015/495) by modified magnetite/H₂O₂, *Chem. Eng. J.* 376 (2019) 120265, <https://doi.org/10.1016/j.cej.2018.10.202>.
- [18] E. Serrano, M. Munoz, Z.M. de Pedro, J.A. Casas, Fast oxidation of the neonicotinoid pesticides listed in the EU Decision 2018/840 from aqueous solutions, *Sep. Purif. Technol.* 235 (2020) 116168, <https://doi.org/10.1016/j.seppur.2019.116168>.
- [19] X. Pan, L. Yan, R. Qu, Z. Wang, Degradation of the UV-filter benzophenone-3 in aqueous solution using persulfate activated by heat, metal ions and light, *Chemosphere* 196 (2018) 95–104, <https://doi.org/10.1016/j.chemosphere.2017.12.152>.
- [20] Y. Zhang, B. Wang, X. Hu, H. Li, Non-activated peroxymonosulfate oxidation of p-aminobenzoic acid in the presence of effluent organic matter, *Chem. Eng. J.* 384 (2020) 123247, <https://doi.org/10.1016/j.cej.2019.123247>.
- [21] S. Tsoumachidou, T. Velegraki, I. Poullos, TiO₂ photocatalytic degradation of UV filter para-aminobenzoic acid under artificial and solar illumination, *J. Chem. Technol. Biotechnol.* 91 (2016) 1773–1781, <https://doi.org/10.1002/jctb.4768>.
- [22] P.M. Perillo, M.N. Atia, C-doped ZnO nanorods for photocatalytic degradation of p-aminobenzoic acid under sunlight, *Nano-Struct. Nano-Objects* 10 (2017) 125–130, <https://doi.org/10.1016/j.nanoso.2017.04.001>.
- [23] M. Munoz, F.J. Mora, Z.M. de Pedro, S. Álvarez-Torrellas, J.A. Casas, J. Rodriguez, Application of CWPO to the treatment of pharmaceutical emerging

- pollutants in different water matrices with a ferromagnetic catalyst, *J. Hazard Mater.* 331 (2017) 45–54, <https://doi.org/10.1016/j.jhazmat.2017.02.017>.
- [24] A.R. Lado Ribeiro, N.F.F. Moreira, G. Li Puma, A.M.T. Silva, Impact of water matrix on the removal of micropollutants by advanced oxidation technologies, *Chem. Eng. J.* 363 (2019) 155–173, <https://doi.org/10.1016/j.cej.2019.01.080>.
- [25] Z. Zhang, Y. Guo, Q. Wang, B. Louis, F. Qi, Heterogeneous Fenton-like reactions with a novel hybrid Cu–Mn–O catalyst for the degradation of benzophenone-3 in aqueous media, *C. R. Chim.* 20 (2017) 87–95, <https://doi.org/10.1016/j.crci.2016.05.014>.
- [26] N. Lopez-Arago, J. Nieto-Sandoval, M. Munoz, Z.M. de Pedro, J.A. Casas, Insights on the removal of the azole pesticides included in the EU watch list by catalytic wet peroxide oxidation, *Environ. Technol. Innov.* 29 (2023) 103004, <https://doi.org/10.1016/j.eti.2022.103004>.
- [27] H. Zúñiga-Benítez, C. Aristizábal-Ciro, G.A. Peñuela, Heterogeneous photocatalytic degradation of the endocrine-disrupting chemical Benzophenone-3: parameters optimization and by-products identification, *J. Environ. Manag.* 167 (2016) 246–258, <https://doi.org/10.1016/j.jenvman.2015.11.047>.
- [28] S. Álvarez-Torrellas, M. Munoz, V. Mondejar, Z.M. de Pedro, J.A. Casas, Boosting the catalytic activity of natural magnetite for wet peroxide oxidation, *Environ. Sci. Pollut. Res.* 27 (2020) 1176–1185, <https://doi.org/10.1007/s11356-018-2171-3>.
- [29] M. Munoz, J. Conde, Z.M. de Pedro, J.A. Casas, Antibiotics abatement in synthetic and real aqueous matrices by H₂O₂/natural magnetite, *Catal. Today* 313 (2018) 142–147, <https://doi.org/10.1016/j.cattod.2017.10.032>.
- [30] C.A. Downs, E. Kramarsky-Winter, R. Segal, J. Fauth, S. Knutson, O. Bronstein, F. R. Ciner, R. Jeger, Y. Lichtenfeld, C.M. Woodley, P. Pennington, K. Cadenas, A. Kushmaro, Y. Loya, Toxicopathological effects of the sunscreen UV filter, oxybenzone (Benzophenone-3), on coral planulae and cultured primary cells and its environmental contamination in Hawaii and the U.S. Virgin Islands, *Arch. Environ. Contam. Toxicol.* 70 (2016) 265–288, <https://doi.org/10.1007/s00244-015-0227-7>.
- [31] Sandell, E.B. Colorimetric Determination of Trace Metals. Interscience Pubs., New York, 1959, <https://doi.org/10.1021/j150441a012>.
- [32] J.J. Pignatello, E. Oliveros, A. MacKay, Advanced oxidation processes for organic contaminant destruction based on the Fenton reaction and related chemistry, *Crit. Rev. Environ. Sci. Technol.* 36 (2006) 1–84, <https://doi.org/10.1080/10643380500326564>.
- [33] F. Stüber, J. Font, A. Eftaxias, M. Paradowska, M.E. Suarez, A. Fortuny, C. Bengoa, A. Fabregat, Chemical wet oxidation for the abatement of refractory non-biodegradable organic wastewater pollutants, *Process Saf. Environ. Prot.* 83 (2005) 371–380, <https://doi.org/10.1205/psep.05017>.
- [34] Q.Q. Cai, M.Y. Wu, R. Li, S.H. Deng, B.C.Y. Lee, S.L. Ong, J.Y. Hu, Potential of combined advanced oxidation – Biological process for cost-effective organic matters removal in reverse osmosis concentrate produced from industrial wastewater reclamation: screening of AOP pre-treatment technologies, *Chem. Eng. J.* 389 (2020) 123419, <https://doi.org/10.1016/j.cej.2019.123419>.
- [35] C. Berberidou, P. Kokkinos, I. Poullos, D. Mantzavinos, Homogeneous photo-fenton degradation and mineralization of model and simulated pesticide wastewaters in lab- and pilot-scale reactors, *Catalysts* 12 (2022) 1512, <https://doi.org/10.3390/catal12121512>.
- [36] J. Nieto-Sandoval, C. di Luca, E. Gomez-Herrero, N. Inchaurredo, M. Munoz, Z. M. de Pedro, J.A. Casas, Innovative iron oxide foams for the removal of micropollutants by catalytic wet peroxide oxidation: assessment of long-term operation under continuous mode, *J. Environ. Chem. Eng.* 9 (2021) 105914, <https://doi.org/10.1016/j.jece.2021.105914>.
- [37] J.H. Ramirez, F.J. Maldonado-Hódar, A.F. Pérez-Cadenas, C. Moreno-Castilla, C. A. Costa, L.M. Madeira, Azo-dye Orange II degradation by heterogeneous Fenton-like reaction using carbon-Fe catalysts, *Appl. Catal. B* 75 (2007) 312–323, <https://doi.org/10.1016/j.apcatb.2007.05.003>.
- [38] M. Munoz, Z.M. de Pedro, J.A. Casas, J.J. Rodriguez, Assessment of the generation of chlorinated byproducts upon Fenton-like oxidation of chlorophenols at different conditions, *J. Hazard. Mater.* 190 (2011) 993–1000, <https://doi.org/10.1016/j.jhazmat.2011.04.038>.
- [39] M. Munoz, Z.M. de Pedro, J.A. Casas, J.J. Rodriguez, Triclosan breakdown by Fenton-like oxidation, *Chem. Eng. J.* 198–199 (2012) 275–281, <https://doi.org/10.1016/j.cej.2012.05.097>.
- [40] H. Zúñiga-Benítez, G.A. Peñuela, Application of solar photo-Fenton for benzophenone-type UV filters removal, *J. Environ. Manag.* 217 (2018) 929–938, <https://doi.org/10.1016/j.jenvman.2018.03.075>.
- [41] Z. Ye, J.R. Steter, F. Centellas, P.L. Cabot, E. Brillas, I. Sirés, Photoelectro-Fenton as post-treatment for electrocoagulated benzophenone-3-loaded synthetic and urban wastewater, *J. Clean. Prod.* 208 (2019) 1393–1402, <https://doi.org/10.1016/j.jclepro.2018.10.181>.
- [42] R. Patidar, V.C. Srivastava, Ultrasound enhanced electro-Fenton mineralization of benzophenone: kinetics and mechanistic analysis, *ACS ES T Water* 3 (2023) 1595–1609, <https://doi.org/10.1021/acsestwater.2c00364>.
- [43] M. Zou, Y. Qi, R. Qu, G. Al-Basher, X. Pan, Z. Wang, Z. Huo, F. Zhu, Effective degradation of 2,4-dihydroxybenzophenone by zero-valent iron powder (Fe⁰)-activated persulfate in aqueous solution: kinetic study, product identification and theoretical calculations, *Sci. Total Environ.* 771 (2021) 144743, <https://doi.org/10.1016/j.scitotenv.2020.144743>.
- [44] J.A. Zazo, J.A. Casas, A.F. Mohedano, M.A. Gilarranz, J.J. Rodríguez, Chemical pathway and kinetics of phenol oxidation by Fenton's reagent, *Environ. Sci. Technol.* 39 (2005) 9295–9302, <https://doi.org/10.1021/es050452h>.
- [45] Y. Luo, W. Guo, H.H. Ngo, L.D. Nghiem, F.I. Hai, J. Zhang, S. Liang, X.C. Wang, A review on the occurrence of micropollutants in the aquatic environment and their fate and removal during wastewater treatment, *Sci. Total Environ.* 473–474 (2014) 619–641, <https://doi.org/10.1016/j.scitotenv.2013.12.065>.
- [46] H. Liu, P. Sun, H. Liu, S. Yang, L. Wang, Z. Wang, Acute toxicity of benzophenone-type UV filters for *Photobacterium phosphoreum* and *Daphnia magna*: QSAR analysis, interspecies relationship and integrated assessment, *Chemosphere* 135 (2015) 182–188, <https://doi.org/10.1016/j.chemosphere.2015.04.036>.
- [47] D. Molins-Delgado, P. Gago-Ferrero, M.S. Díaz-Cruz, D. Barceló, Single and joint ecotoxicity data estimation of organic UV filters and nanomaterials toward selected aquatic organisms. Urban groundwater risk assessment, *Environ. Res.* 145 (2016) 126–134, <https://doi.org/10.1016/j.envres.2015.11.026>.
- [48] Y. Du, W.Q. Wang, Z.T. Pei, F. Ahmad, R.R. Xu, Y.M. Zhang, L.W. Sun, Acute toxicity and ecological risk assessment of benzophenone-3 (BP-3) and benzophenone-4 (BP-4) in ultraviolet (UV)-filters, *Int. J. Environ. Res. Public Health* 14 (2017) 1414, <https://doi.org/10.3390/ijerph14111414>.
- [49] Q. Zhang, X. Ma, M. Dzakpasu, X.C. Wang, Evaluation of ecotoxicological effects of benzophenone UV filters: luminescent bacteria toxicity, genotoxicity and hormonal activity, *Ecotoxicol. Environ. Saf.* 142 (2017) 338–347, <https://doi.org/10.1016/j.ecoenv.2017.04.027>.
- [50] Y. Huacalco-Aguilar, S. Álvarez-Torrellas, M.V. Gil, M. Larriba, J. García, Insights of emerging contaminants removal in real water matrices by CWPO using a magnetic catalyst, *J. Environ. Chem. Eng.* 9 (2021) 106321, <https://doi.org/10.1016/j.jece.2021.106321>.
- [51] R.S. Ribeiro, Z. Frontistis, D. Mantzavinos, D. Venieri, M. Antonopoulou, I. Konstantinou, A.M.T. Silva, J.L. Faria, H.T. Gomes, Magnetic carbon xerogels for the catalytic wet peroxide oxidation of sulfamethoxazole in environmentally relevant water matrices, *Appl. Catal. B* 199 (2016) 170–186, <https://doi.org/10.1016/j.apcatb.2016.06.021>.
- [52] X. Li, B. Yang, K. Xiao, H. Duan, J. Wan, H. Zhao, Targeted degradation of refractory organic compounds in wastewaters based on molecular imprinting catalysts, *Water Res.* 203 (2021) 117541, <https://doi.org/10.1016/j.watres.2021.117541>.
- [53] C. Yu, Z. Zhao, Y. Zong, L. Xu, B. Zhang, D. Wu, Electric field-enhanced coupled with metal-free peroxymonosulfate activator: the selective oxidation of nonradical species-dominated system, *Water Res* 227 (2022) 119323, <https://doi.org/10.1016/j.watres.2022.119323>.
- [54] D.B. Miklos, C. Remy, M. Jekel, K.G. Linden, J.E. Drewes, U. Hübner, Evaluation of advanced oxidation processes for water and wastewater treatment – a critical review, *Water Res.* 139 (2018) 118–131, <https://doi.org/10.1016/j.watres.2018.03.042>.
- [55] D. Ortiz, M. Munoz, S. Cirés, J.L. Arribas Mediero, M.C. Crisostomo, A.C. Forero Ortiz, Z.M. de Pedro, F. Rogalla, A. Quesada, J.A. Casas, Influence of the aqueous matrix on the degradation of cyanotoxins by CWPO: a study on the Iberian Peninsula freshwaters, *J. Environ. Chem. Eng.* 11 (2023) 110581, <https://doi.org/10.1016/j.jece.2023.110581>.